Numerical Simulations of Chaotic Dynamics in a Model of an Elastic Cable*

F. BENEDETTINI and G. REGA

Dipartimento di Ingegneria delle Strutture, delle Acque e del Terreno, Università dell'Aquila, Monteluco Roio, 67040 L'Aquila, Italy

Abstract. The finite motions of a suspended elastic cable subjected to a planar harmonic excitation can be studied accurately enough through a single ordinary-differential equation with quadratic and cubic nonlinearities.

The possible onset of chaotic motion for the cable in the region between the one-half subharmonic resonance condition and the primary one is analysed via numerical simulations. Chaotic charts in the parameter space of the excitation are obtained and the transition from periodic to chaotic regimes is analysed in detail by using phase-plane portraits, Poincaré maps, frequency-power spectra, Lyapunov exponents and fractal dimensions as chaotic measures. Period-doubling, sudden changes and intermittency bifurcations are observed.

Key words: numerical simulation, chaos, cable, resonances, bifurcations.

1. Introduction

Some papers, both numerical and analytical, appeared recently in the literature on the subject of nonlinear vibrations of suspended elastic cables, which are of interest in several technical applications. Most of them deal with a single cable for which simple models, with one or two degrees-of-freedom, have been developed and used to obtain an analytical solution of the problem and an effective description of the nonlinear dynamic behaviour. Free planar and nonplanar motions were studied widely [1–3], while relatively few works were devoted to forced motions [4–6]. The main features of the relevant dynamical problems are associated with the presence of both quadratic and cubic nonlinearities in the equations of motion, the former is due to the cable initial curvature and the latter is due to stretching of the cable axis. Among the various interesting phenomena occurring at finite vibration amplitudes for cables with different sag-to-span ratios, the subharmonic or superharmonic motions of the system taking place in the neighbourhood of the secondary resonance conditions are worth mentioning.

Since the 'strange' behaviour of dynamical systems is often associated with the loss of stability of secondary responses [7–8], which leads to bifurcations and eventually to chaos in certain ranges of values of the system parameters, there is strong technical interest in the analysis and understanding of possible chaotic regimes for suspended cables.

Interest in the analysis of the chaotic behaviour of dynamical systems has been strongly increasing in the last decade [9–10]. The existence of strange attractors was demonstrated in the literature for systems described by several nonlinear equations. In structural dynamics, the stable and unstable Duffing equations [11] governing the finite vibrations of taut strings or beams and, respectively, of periodically forced buckled beams are of main interest. They exhibit only a symmetric (cubic) nonlinear term. Instead, the equation with quadratic and cubic nonlinearities

* Part of this work was presented at the XVIIth Int. Congr. of Theor. and Appl. Mech., Grenoble, August 1988.

Nonlinear Dynamics **1**: 23–38, 1990

has received minor attention from the chaotic dynamics viewpoint [7, 8, 12], though the possible routes to chaos can be traced in the work of Szemplinska-Stupnicka. Yet, this equation is interesting both for describing the dynamic behaviour of various structural elements (curved beams, shallow arches, suspended cables) and for exhibiting a non-symmetric nonlinear term.

The present work is just concerned with the possible onset of chaotic motions for an elastic cable subjected to a planar harmonic forcing. Using a one-degree-of-freedom model based upon an approximation to the cable shape during the motion, we performed numerical simulations of the planar periodic and chaotic responses for an actually suspended cable by varying the amplitude and frequency of the excitation in the region between the one-half subharmonic resonance condition and the primary one. Of course, restriction of the motions to one plane is a limitation to the problem examined. However, it is worth mentioning that, theoretically speaking, the in-plane oscillations produced by a planar excitation do not force out-of-plane oscillations, due to the nature of the modal coupling [1].

Different dynamical measures are used to identify chaos, such as phase-plane portraits, Poincaré maps, frequency-power spectra, Lyapunov exponents and fractal dimensions. Chaotic regions in the control parameter space of the problem are obtained and the transitions from periodic to chaotic motions of the system are analysed in detail. Some points concerning the computational aspects associated with the use of the various measures are also discussed in the paper.

2. Equation of Motion and Periodic Solutions

A parabolic elastic cable suspended between two fixed supports at the same level is considered (Figure 1). Let EA, H and m be the axial rigidity, the initial tension and the mass per unit length of the cable, respectively. Under the assumption of moderately large rotations of the cable element in the motion around the initial static equilibrium configuration $y(x)$ and of negligible horizontal inertia forces, the cable dynamics can be described by the unique partial integro-differential equation in the vertical displacement $v(x, t)$ [5]

$$\left\{Hv' + (EA/l)\cdot(y' + v')\int_0^l [y'v' + v'^2/2]\,\mathrm{d}x\right\}' + p - \mu\dot{v} = m\ddot{v}\,, \tag{1}$$

where the prime and the dot stand for $\partial/\partial x$ and $\partial/\partial t$, respectively, $p(x, t)$ is a vertical distributed load and μ is a viscous damping coefficient per unit length.

Equation (1) is accurate for studying suspended cables used in overhead transmission lines for which the sag-to-span ratio $d/l \cong 1/20$, $H/EA = 0[(d/l)^2]$ and the dynamical displacement

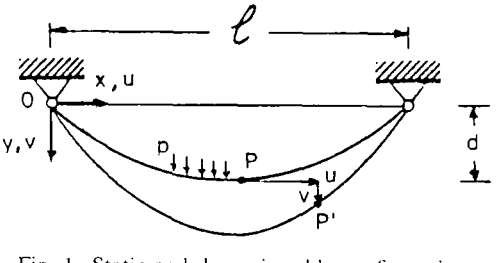

Fig. 1. Static and dynamic cable configurations.

components are respectively $u = 0(\varepsilon d^2/l)$ and $v = 0(\varepsilon d)$, with ε being a small parameter of the order of the amplitude.

The following nondimensional variables are introduced:

$$\tilde{x} = x/l, \quad \tilde{t} = \omega t, \quad \tilde{v} = v/l, \quad \tilde{\mu} = \mu\omega l^2/H, \quad \tilde{p} = pl/H\,, \tag{2}$$

where ω is the linear frequency of a generic vibration mode of the cable. By representing the displacement through one linear eigenfunction $f(x)$ [13] and considering a monofrequency harmonic excitation with given spatial distribution $\psi(x)$,

$$\tilde{v}(x, t) = f(x)q(t), \quad \tilde{p}(x, t) = \psi(x)P\cos\Omega t\,, \tag{3}$$

one can apply the Galerkin method to equation (1) and arrive at the following single ordinary-differential equation of motion:

$$\ddot{q} + \mu^*\dot{q} + q + c_2q^2 + c_3q^3 = p^*\cos\Omega t. \tag{4}$$

It exhibits both quadratic and cubic nonlinearities, with the coefficients c_2 and c_3 depending on the cable properties and the shape functions considered. Using a different nondimensionalization for the displacement, we obtained [5] approximate steady-state solutions to equation (4) in the neighbourhood of the primary resonance condition ($\Omega \cong 1$) for various cables by a fourth-order perturbation procedure. Though the features of the response vary notably with the cable sag-to-span ratio, the ensuing motion of the system in this frequency range firmly has a normalized period equal to 1.

Moreover, using just the same nondimensionalization for the displacement as considered herein, we obtained [6] approximate steady-state solutions to equation (4) in the neighbourhood of the subharmonic resonance of order one half ($\Omega \cong 2$) by a second-order perturbation approach. Regions of existence or non-existence of finite-amplitude stable subharmonic oscillations with period 2 were obtained in the parameter space (Ω, p) of the excitation. For prestressed cables subjected to uniform forcing and vibrating with the first symmetric mode, which is the first mode of a cable with sag-to-span ratio up to about 1/20 and technical values of EA/H ($\cong$500), those regions are plotted in Figure 2, where the thick lines refer to a nearly taut cable ($d/l \cong 1/145$) and

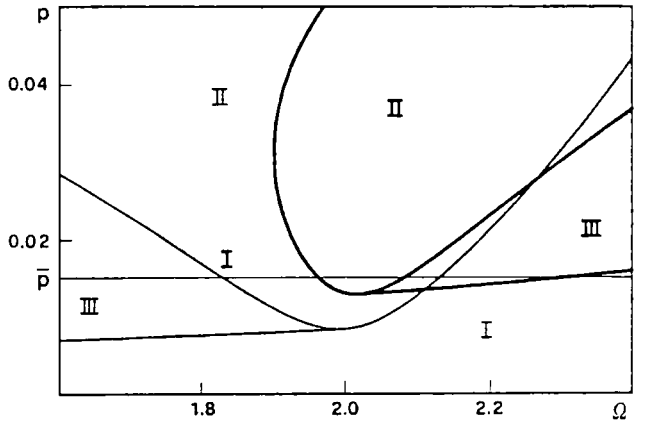

Fig. 2. Regions of non-existence (I), existence (II) and possible existence (III) of period 2 motions for a nearly taut (thick) and a sagged (thin) cable, perturbation results, $\mu = 0.1$.

the thin lines to a sagged cable ($d/l \cong 1/45$). Regions I, II and III are, respectively, regions of non-existence, existence and possible existence of finite-amplitude subharmonic oscillations, depending on the initial conditions.

In the case of a sagged cable that exhibits a frequency-response curve of the softening type, the approximate solution shows possible existence of a finite response with period 2 at frequencies notably less than the subharmonic-resonance value, a physically unrealistic behaviour which may be due to the order considered in the perturbation analysis [6]. Indeed, some numerical integrations of equation (4) showed that, when decreasing Ω with $p = \bar{p}$ and fixed initial conditions ($q = \dot{q} = 0$), the response is actually of period 2 up to a certain frequency ($\Omega \cong 1.7$) and then it becomes of period 1, as one would expect since the fundamental harmonic firmly prevails in the response right of the primary resonance condition. Thus the question arises of what is the kind of motion that actually develops in the region between the one-half subharmonic ($\Omega \cong 2$) and primary ($\Omega \cong 1$) resonances of the system.

Moreover, since transition to chaotic motions has been recently observed for an oscillator with quadratic and cubic nonlinearities in the neighbourhood of the 1/2 subharmonic resonance [7, 8], there is strong interest in examining the possible onset of such irregular responses for the present system.

3. Measures for Chaos and Computational Aspects

To answer these questions, we made extensive numerical simulations of the solutions of equation (4) by considering values of the coefficients of the nonlinear terms ($c_2 = 35.952$, $c_3 = 534.53$) relevant to the above mentioned sagged cable. The amplitude and frequency of the excitation are varied parametrically and, to a smaller extent, the damping ratio too. As a rule, the initial conditions are held fixed ($q = \dot{q} = 0$), except for some system parameter values for which the domains of attraction of different solutions are investigated.

To identify the type of response with reasonable accuracy, we used different dynamical measure, of both qualitative and quantitative nature, whenever there is a doubt of chaotic behaviour [10]. Namely, besides the time history whose irregular shape is not a foolproof test for chaos, phase plane portraits, Poincaré maps, frequency-power spectra, Lyapunov exponents and fractal dimensions are used.

Obtaining reliable results with each measure needs preliminary calibration of some computational parameters. The numerical integration of the equation of motion has been made through a fourth-order Runge–Kutta method and checked through the Adams variable step method. Different total integration time lengths (up to 4000 forcing periods) and time-step increments (up to 1/800 of the forcing period) have been considered to be reasonably sure that the response obtained is really a steady one and that chaos, whether occurring, actually pertains to the differential equation of motion and not to a difference approximation of it [14]. The length of the initial transient and its influence on the response have been carefully checked. When using the FFT for generating power spectra, we have considered at least 120 forcing periods.

Lyapunov exponents characterize quantitatively the average exponential divergence or convergence of nearby trajectories. They are determined by examining the long-time evolution of an infinitesimal n-sphere of initial conditions of radius d_0, where n is the order of the nonlinear system. Under the flow, the sphere is mapped into an ellipsoid with n principal axes $d_i(t)$ and there is a spectrum of Lyapunov exponents defined by the relationship [15]

$$\lambda_i = \lim_{t\to\infty} \frac{1}{t} \log_2 \frac{d_i(t)}{d_0} \,. \tag{5}$$

Negative exponents denote periodic orbits while the presence of at least one positive exponent indicates stretching of the sphere in one direction and thus divergence of initially close trajectories. For the third-order autonomous system

$$\begin{aligned} \dot{x}_1 &= x_2 \,, \\ \dot{x}_2 &= -\mu x_2 - x_1 - c_2 x_1^2 - c_3 x_1^3 + p\cos\phi \,, \\ \dot{\phi} &= \Omega \,, \end{aligned} \tag{6}$$

into which equation (4) (with the stars omitted) can be transformed through the positions $x_1 = q$, $x_2 = \dot{q}$, $\phi = \Omega t$, the two non-zero exponents λ_1 and λ_2 (the third one λ_3 along the flow being zero) have been calculated by means of a now classical algorithm [15] based on the simultaneous integration of the system of nonlinear differential equations (6) and of the corresponding linearized equations.

Among the various measures of fractal dimension proposed in the literature to quantify the strangeness of an attractor [10], reference is made here to the Lyapunov dimension D_L and the correlation dimension D_c. The first choice naturally arises after the calculation of the exponents, from which that measure can readily be obtained according to a conjecture by Kaplan and Yorke [16]. In the present case, in which the dimension refers to the two-dimensional set of points generated by a Poincaré map of the third-order set of differential equations (6), it is simply calculated as

$$D_L = 1 - \lambda_1/\lambda_2 \,. \tag{7}$$

As a second measure to be compared with the previous one, the correlation dimension proposed by Grassberger and Proccacia [17] is used, both for being well suited to time sampled data, such as those of a Poincaré map, and for accounting for the frequency with which the trajectory visits various regions of the attractor, thus being more effective than a merely geometric measure of a set of N points [10]. It is defined as:

$$D_c = \lim_{r\to 0} \frac{\log C(r)}{\log r} \,, \tag{8}$$

where r is the radius of a two-dimensional box centered at each point $\mathbf{x}_i = \{q_i, \dot{q}_i\}$ of the set and $C(r)$ is the correlation function

$$C(r) = \frac{1}{N^2} \sum_i^N \sum_j^N H(r - |\mathbf{x}_i - \mathbf{x}_j|) \tag{9}$$

which is calculated by counting the number of points in each box, assuming $H(s) = 1$ if $s \geqslant 0$ and $H(s) = 0$ if $s < 0$.

For the selection of the algorithmic parameters playing a role in the response of chaotic systems, e.g. the time step increment to be used in extended numerical investigations, useful suggestions can be obtained from the analysis of the values assumed in some sample cases by

global quantitative measures of the system dynamics, like the Lyapunov exponents and the dimension of the attractor. Of course, use of these measures too needs computational care. As far as the Lyapunov exponents are concerned, problems may arise both in the selection of the fixed but arbitrary time interval of renormalization of the vector identifying a nearby trajectory [15] and in the determination of the number of forcing periods to be used for obtaining well stabilized values of the exponents. On the other hand, a reliable calculation of the correlation dimension of the attractor in the Poincaré map, besides being more time consuming than that of the exponents, must pay attention to the minimum and maximum dimensions considered for the box: these have to be properly correlated with the density of points in the map, since the dimension must be calculated by considering only the r domain in which the log $C(r)$ versus log r ratio is linear [10]. However, once these aspects have been made clear and the time integration length has been chosen in such a way to be representative enough of a non-transient chaotic response, these global dynamical measures prove to be successful for setting the time step increment, whose value can be selected so as to obtain well stabilized values of D_c or of the exponents. From this last view point, it is worth noting that the λ values do not vary any more after few hundreds of forcing periods, while the D_c values usually need more than a thousand periods to remain unchanged.

4. Results

Attention is focused on the following practical aspects:
- determination of significant regions of chaotic response of the system in the control parameters space of the dynamic problem;
- analysis of the system's bifurcations from periodic to chaotic motions.

Some points on the use of the different measures of the dynamics for identifying chaotic responses are also made.

4.1. Regions of periodic and chaotic motions

Figure 3 shows the types of responses found in the neighbourhood of the 1/2-subharmonic resonance of the system for different values of the forcing amplitude; it was obtained by using a time step increment equal to 1/200 and by considering 2000 forcing periods. Small dots denote periodic responses while thick dots denote chaotic responses. Some regions with well-established period 1 or period 2 responses are clearly evident. The boundary curve obtained numerically (thick line) and separating the lower region of period 1 motions from that of period 2 motions shows good qualitative agreement with the boundary curves (thin lines) obtained using the second-order perturbation solution (see Figure 2). For a correct comparison, we note that the numerical results refer in any case to zero initial conditions while the two perturbation curves on the left of the resonance bound a region where period 2 responses may or may not occur, depending on the initial conditions considered.

The more interesting result emerging from the chart in Figure 3 is the occurrence of a rather large region of chaotic motions between the two regions of periodic motions. Although its presence might be predicted from the findings in [7], it is worth noting that the excitation levels in the chaotic region are little higher than the threshold excitaton level for obtaining a period 2 response. Thus, for the cable, due to the high values of the nonlinear coefficients, chaos develops at values of the forcing amplitude notably lower than those in [7], which is of practical interest. As

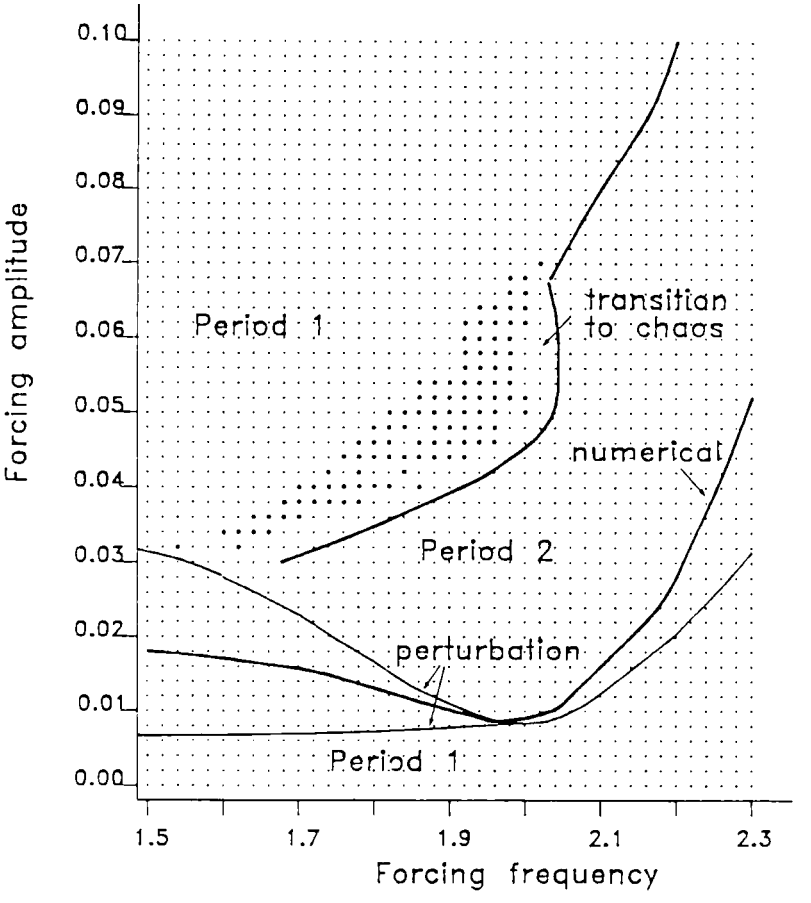

Fig. 3. Regions of periodic (· · ·) and chaotic (· · ·) motions, numerical results, $\mu = 0.1$.

the forcing amplitude increases, the region of period 1 response extends notably to the right, contrary to the prediction of the second-order subharmonic perturbation solution [6] and consistent with the fourth-order primary perturbation solution [5], which predicts more and more pronounced bending to the right of the frequency-response curve with increasing excitation amplitude.

Close to the right neighbourhood of the chaotic region, a band of parameter values where regular motions with period other than 2 occur is found. This band is labelled as transition to chaos in Figure 3. However, the scale of mesh spacing used ($\Delta\Omega = 0.02$, $\Delta p = 0.002$) does not allow us to understand the mechanism of such a transition.

So, for a fixed value of the amplitude ($p = 0.04$), a much finer mesh spacing is considered for the frequency ($\Delta\Omega = 0.0001$). Figure 4a shows the kind of steady-state motions obtained, as inferred from the Poincaré maps and the power spectra: the periodicity of the output (period 1, period 2, etc.) is recorded as a function of frequency. Figure 4b shows the corresponding variations of the two Lyapunov exponents of the dynamical system. They were calculated by using a total time length of the trajectory equal to 500 forcing periods, which corresponds to well stabilized values of the exponents, and by performing the required orthonormalization at each time step of the integration. Notwithstanding they were obtained with a larger frequency mesh spacing ($\Delta\Omega = 0.001$) and a number of forcing periods notably lower than those used for obtaining

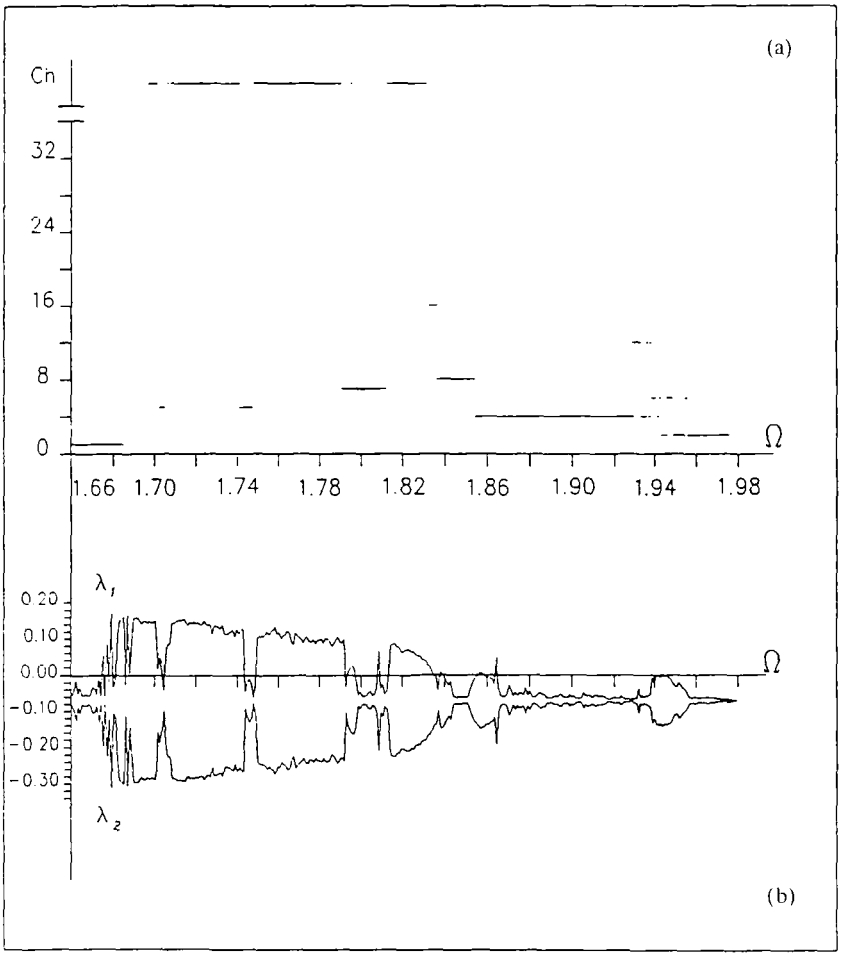

Fig. 4. Periodicity of the steady state motions as a function of the forcing frequency (a) and spectrum of the associated Lyapunov exponents (b), $p = 0.04$, $\mu = 0.1$.

Figure 4a, a very good qualitative agreement with the indications given by the measures of chaos used therein is observed. Namely, the first exponent is positive in the chaotic zones and negtive in practically all zones where the Poincaré map and power spectrum indicate a periodic response of the system. In substance, the spectrum of the Lyapunov exponents obtained by varying a control parameter proves to be a powerful tool for obtaining bifurcation diagrams [18, 19]. This is clearly shown by the sequence of spectra reported in Figures 5a–d, which refer to four increasing levels of the excitation within the region of chaotic response. Consistent with Figure 3, the overall chaos zone progressively shifts towards higher frequency values.

Nevertheless, the algorithmic aspects make construction of bifurcation diagrams through Lyapunov exponents more time consuming than through observation of the Poincaré maps. Moreover, the latter dynamical measure is a more complete one, since it allows one to understand more effectively the mechanism of transition from periodic to chaotic motions. In the next section, the main features of the system response, as far as the kinds of periodic solutions and of bifurcations occurring are concerned, will be examined just by using the Poincaré map as a principal indicator.

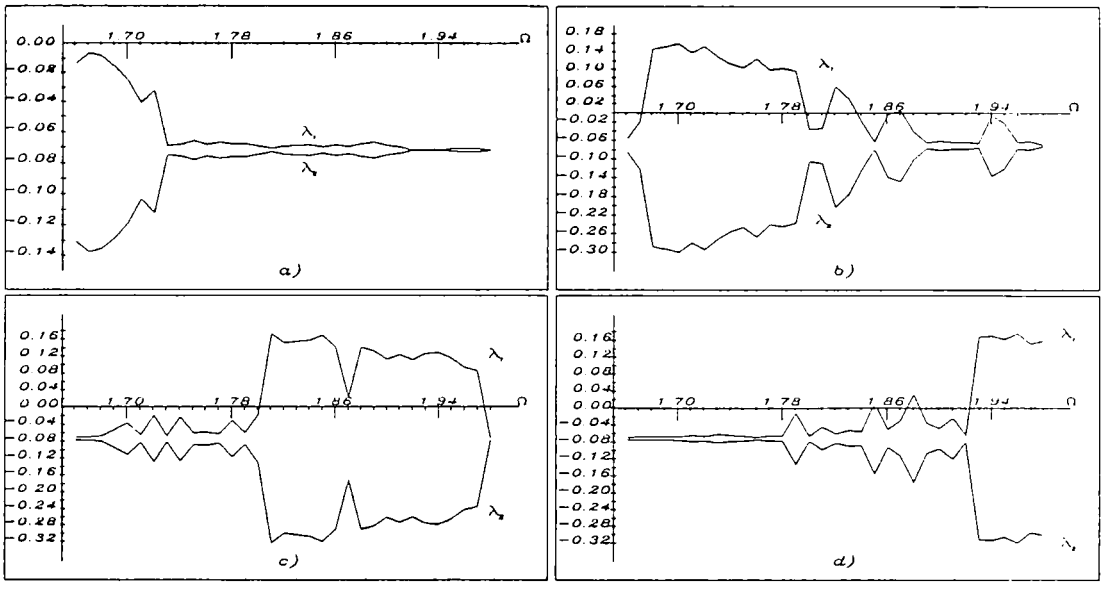

Fig. 5. Spectrum of the exponents as a tool for localizing chaos zones at different values of the forcing amplitude.

4.2. Bifurcations and chaos

By examining the results obtained at $p = 0.04$ with decreasing frequency, a main route to chaos through period-doubling bifurcations is clearly observed [7]. Responses with periods 2, 4, 8, 16 are shown in Figures 6a–d, in each of which the phase plane portrait, the Poincaré map and the frequency-power spectrum are reported. The first two indicators show the successive splitting of the trajectories and of the isolated points respectively, as the bifurcation progresses. At each step, new lines appear in the power spectrum (plotted with logarithmic scale) at the midpoints of the frequency intervals between the peaks of the previous spectrum. As Ω decreases further, the points in the Poincaré map first gather along line segments (Figure 7a) and then diffuse in the plane though remaining restricted to a well defined region, which is the strange attractor of the system (Figure 7b). Correspondingly, a substantially continuous spectrum is achieved. The values of the Lyapunov exponents and the Lyapunov and correlation dimensions indicate that the last two responses are chaotic, though their Poincaré maps and fractal dimensions are different. We note that D_c is lower than D_L, as demonstrated in the literature [10], and its numerical value must be carefully checked when close to unity.

The transition to chaos is smooth, namely it occurs in a rather large range of frequency values, and each new periodic solution of the sequence is stable in a smaller interval than the previous one (see Figure 4). Once developed, the chaotic behaviour occurs in a quite large region. The indicators for a well-established chaotic response are shown in Figure 8.

Some points are worth mentioning as far as the fractal dimension of the strange attractor is concerned; D_c was calculated by considering 2000 points in the two-dimensional Poincaré map and approximately three points per box for the lower value of r. It is furnished by the slope of the regression line passing through the points giving the values of the correlation function $C(r)$ corresponding to different values of the box radius [10]. In Figure 9 these lines are plotted for three different values of damping and the relevant values of the dimension are reported. As

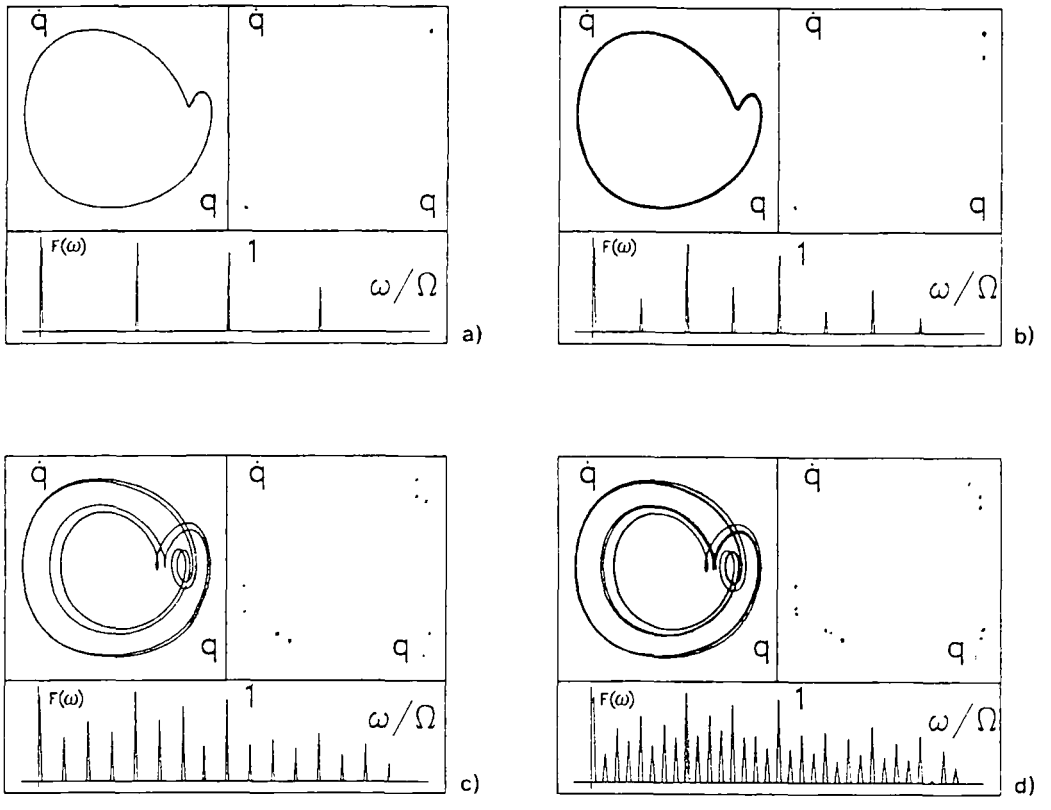

Fig. 6. Period doubling bifurcations: motions with period 2 (a, $\Omega = 1.9475$), 4 (b, $\Omega = 1.945$), 8 (c, $\Omega = 1.840$), 16 (d, $\Omega = 1.836$).

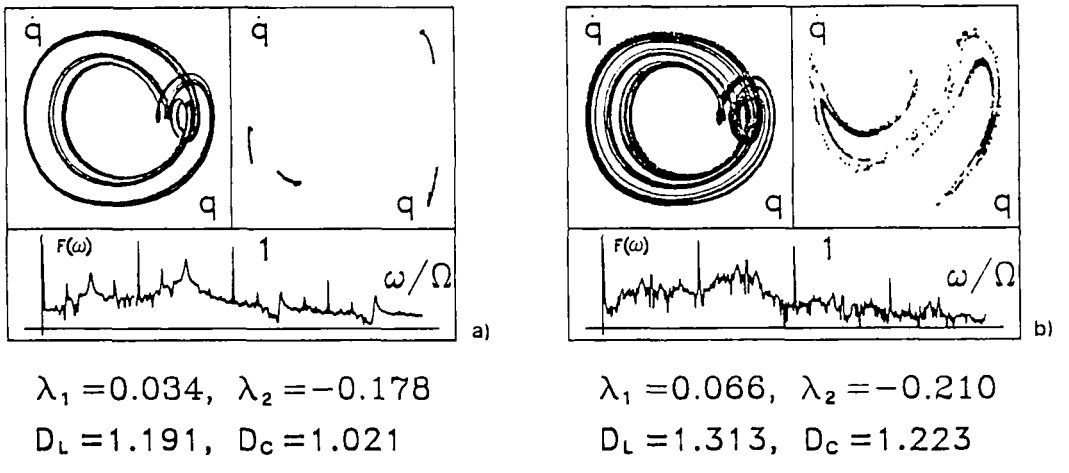

Fig. 7. Indicators for different chaotic responses: (a) $\Omega = 1.830$, (b) $\Omega = 1.820$.

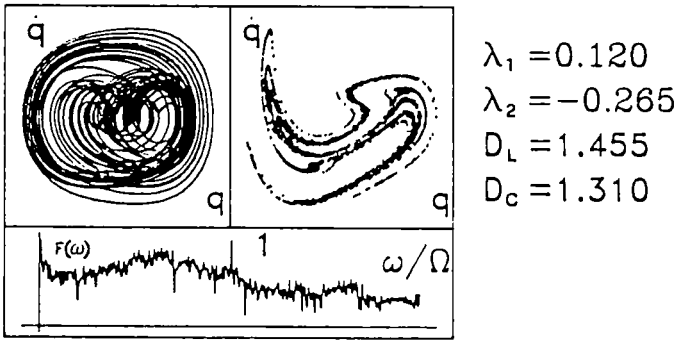

Fig. 8. Well-established chaos, $\Omega = 1.740$.

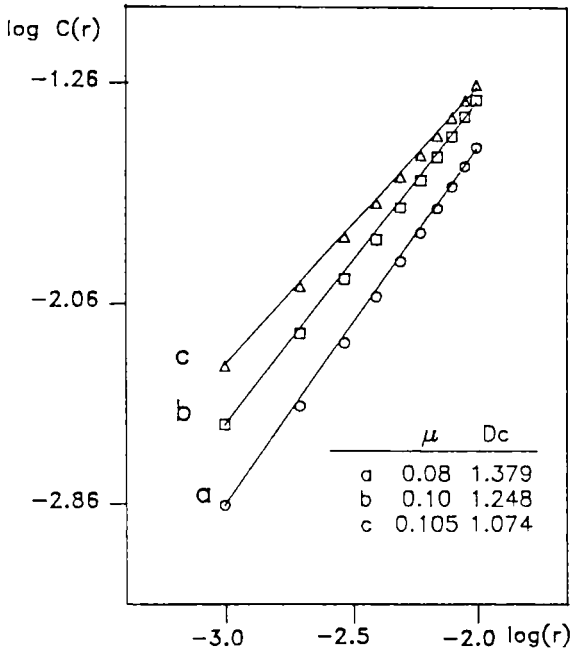

Fig. 9. Correlation dimension of the two-dimensional strange attractor for different damping values, $p = 0.05$, $\Omega = 1.90$.

expected, D_c diminishes with increasing values of μ, which give rise to thinner and thinner strange attractors in the Poincaré map (Figure 10).

For given values of all system parameters, the shape of the Poincaré map changes with the phase ϕ of the forcing function with which one stroboscopically produces the map, as shown in Figure 11, but D_c remains practically unchanged. This allows us [10, 20] to calculate the fractal dimenson of the chaotic attractor in the three-dimensional phase space $(q, \dot{q}, \phi)$ simply as $d_c = 1 + D_c$. In the reference case considered the value $d_c \cong 2.36$ is obtained.

Coming back to the sequence of bifurcations occurring in the frequency range examined, some more periodic solutions are observed both prior and after the establishment of chaos (Figure 4). In particular, as the frequency decreases, responses with period 6 (Figure 12a), 7 (Figure 12b) and 5 (Figure 12c) are observed, which are qualitatively different from both the period 2 response

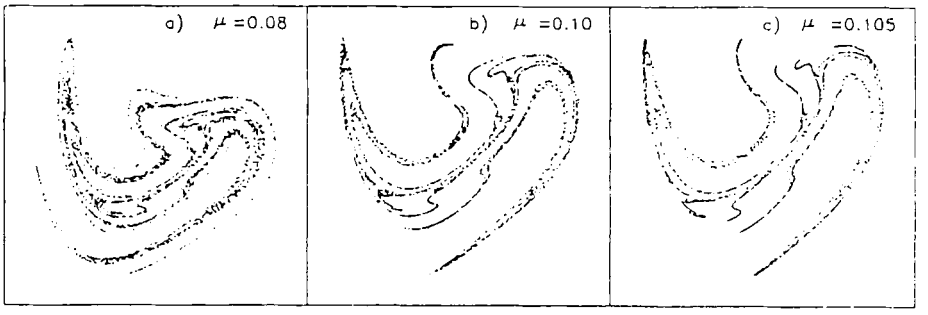

Fig. 10. Poincaré section for different damping values, $p = 0.05$, $\Omega = 1.90$.

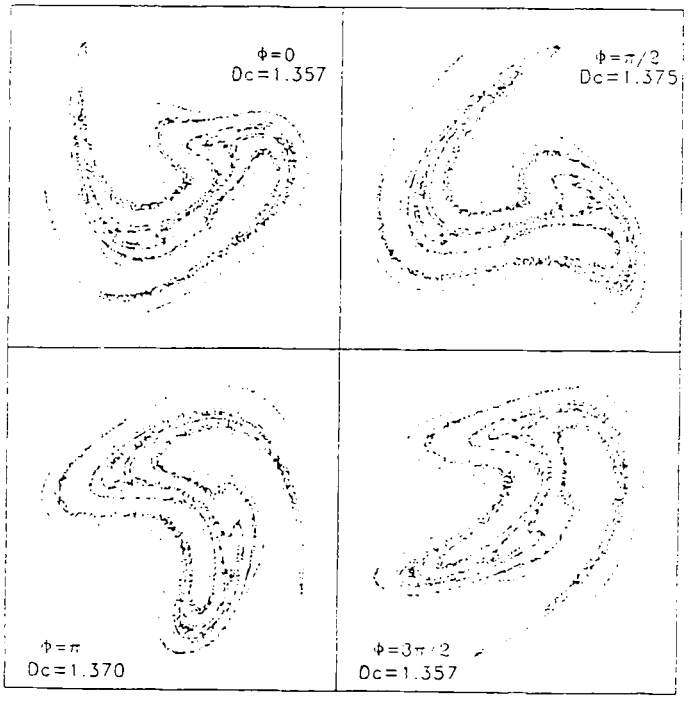

Fig. 11. Poincaré section and correlation dimension for different phase values of the forcing function, $\mu = 0.08$, $p = 0.05$, $\Omega = 1.90$.

(Figure 6a) occurring on the right of the chaotic region and from the period 1 response (Figure 12d) on its left. These solutions are stable in very small intervals. They look like basic responses giving rise to further independent sequences of period-doubling bifurcations (6–12, 7–14, 5–10–20 respectively) occurring in the region examined, like those reported in the literature for other dynamical problems [11, 21]. Unlike the results in [11], however, these independent period-doubling bifurcations are obtained here with fixed values of a control parameter of the system and of the initial conditions. With the frequency spacing considered, these sequences of period doublings seem to be incomplete and the transitions to chaos, where occurring, are observed to be jump phenomena, just as in the cases discussed in [21].

A more precise characterization of the whole sequence of bifurcations taking place would require deeper numerical and theoretical investigations, in which attention should be paid to some

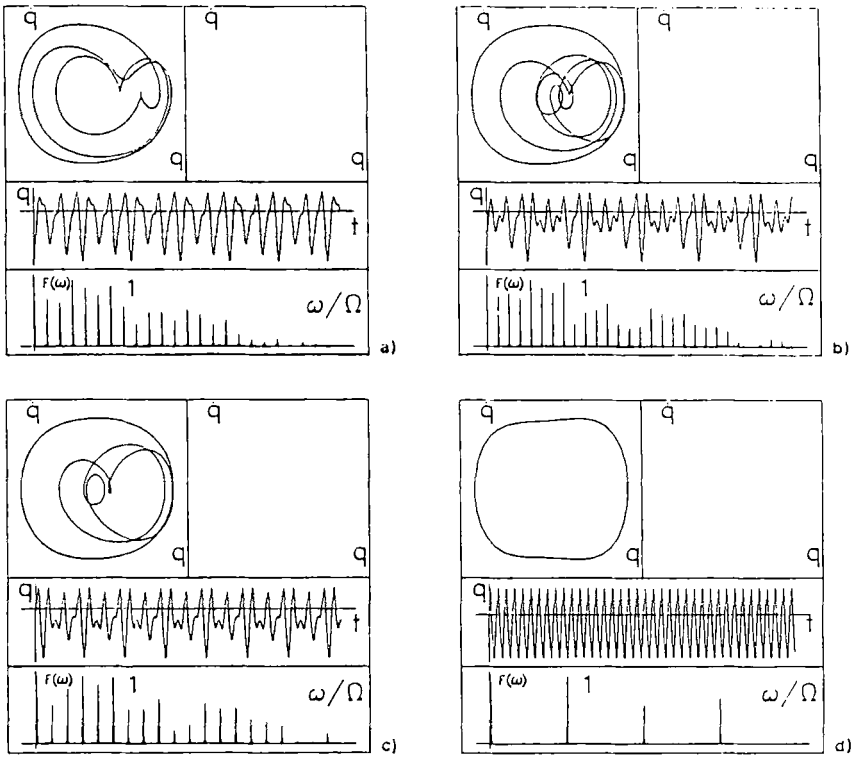

Fig. 12. Other periodic motions: period 6 (a, $\Omega = 1.959$), 7 (b, $\Omega = 1.800$), 5 (c, $\Omega = 1.745$), 1 (d, $\Omega = 1.640$); $p = 0.04$, $\mu = 0.1$.

routes to chaos illustrated in the literature for similar mathematical or physical systems, e.g. the Sarkowski sequence [22] and the subharmonic route to turbulence [23]. However, what is interesting from a practical point of view is that very small variations in a control parameter can influence strongly the type of response of the system, which is a consequence of the fractal nature of the region of chaos.

As the frequency decreases further, the left boundary of this region is approached (Figure 4) and the transition to the stable period 1 motions occurs via a sudden change (jump) of the type just discussed. This result is consistent with the sharp transition found on the left of the chaos region in [8]. Nevertheless, a more detailed investigation of what happens in the neighbourhood of this left boundary ($1.695 < \Omega < 1.70$, Figure 13), made with a frequency spacing $\Delta\Omega = 0.00001$ and

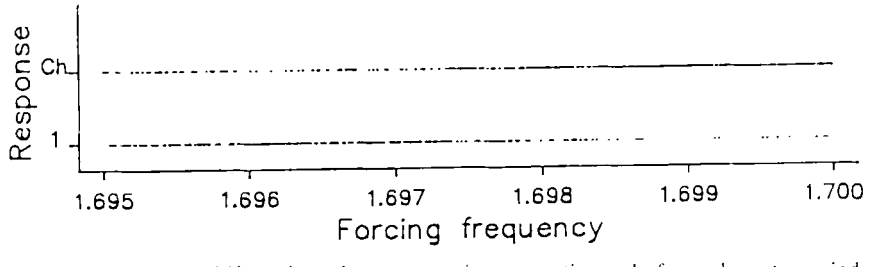

Fig. 13. Sudden change bifurcation: the response jumps continuously from chaos to period 1.

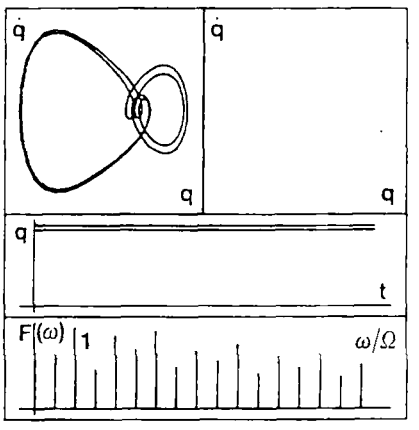

a)

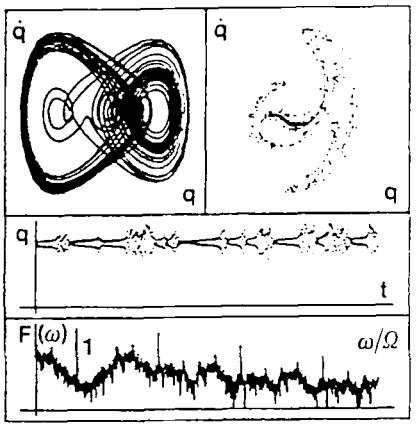

b)

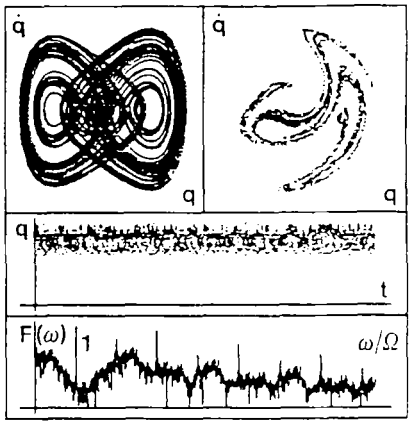

c)

Ω	1.570	1.569
λ_1	0.143	0.180
λ_2	-0.288	-0.325
D_L	1.498	1.555

Fig. 14. Intermittency bifurcation to chaos, $p = 1.77$, $\mu = 0.1$, $\Omega = 1.571$ (a), 1.570 (b), 1.569 (c).

a time step increment equal to 1/400, shows that transition to period 1 motions develops in a finite width zone in which the response continuously jumps from chaotic to period 1. As the frequency is decreased, the chaotic intervals become smaller and smaller while the period 1 intervals extend progressively. This behaviour of the system is to be connected again with the fractal nature of the boundary of the chaotic region, according to which different attractors coexist and the response becomes totally unpredictable – and qualitatively much variable – in this range of frequency.

As a final point, it is worth noting that some other regions of chaotic behaviour were found at greater values of the excitation amplitude. They were not investigated in detail because they are of low technical interest, just due to the high forcing amplitudes involved. Nevertheless, from a theoretical point of view, the occurrence of yet another type of transition to chaos for the equation with quadratic and cubic nonlinearities being considered is worth observing. Namely, with $p = 1.77$ and Ω decreasing from 1.571 to 1.569, the response bifurcates from a period 2 to a well-established chaotic one via intermittency (Figures 14a–c). This is clearly revealed by the intermediate diagram of Figure 14b – a Poincaré map in the t–q plane – which exhibits intervals of nearly period 2 motions and sudden bursts of chaotic behaviour. Of course, the response in Figure 14b was found to be steadily intermittent.

5. Concluding Remarks

The numerical simulations showed that chaotic responses can occur for a suspended elastic cable subjected to a planar monofrequency excitation in the range of frequency between primary and one-half subharmonic resonance.

Careful use of various qualitative and quantitative measures of chaotic dynamics furnished convincing evidence about the actual character of the responses obtained. A chaotic chart and bifurcation diagrams were built in the control parameter space of the system and the fractal properties of the strange attractors were quantified. Different kinds of transition from periodic to chaotic motions were observed, namely via period-doubling bifurcations and sudden change or intermittency bifurcations. Coexistence of different periodic and chaotic motions was observed for many values of the control parameters, consistent with the fractal-like nature of the chaotic region. The ensuing unpredictability of the type of response of the system has to be properly accounted for in technical applications, when one desires to perfectly control it or wants to avoid chaotic regimes in its behaviour.

Acknowledgement

This research was partially supported by M.P.I. 40% – 1988 Grants.

References

1. Benedettini, F., Rega, G., and Vestroni, F., 'Modal coupling in the free nonplanar finite motion of an elastic cable', *Meccanica* **21**, 1986, 38–46.
2. Luongo, A., Rega, G., and Vestroni, F., 'On large-amplitude vibrations of cables', *J. Sound Vibrat.* **116**, 1987, 573–575.
3. Takahashi, K. and Konishi, Y., 'Non-linear vibrations of cables in three dimensions, Part I: Non-linear free vibrations', *J. Sound Vibrat.* **118**, 1987, 69–84.
4. Takahashi, K. and Konishi, Y., 'Non-linear vibrations of cables in three dimensions, Part II: Out-of-plane vibrations under in-plane sinusoidally time-varying load', *J. Sound Vibrat.* **118**, 1987, 85–97.
5. Benedettini, F. and Rega, G., 'Nonlinear dynamics of an elastic cable under planar excitation', *Int. J. Non-Linear Mech.* **22**, 1987, 497–509.
6. Rega, G. and Benedettini, F., 'Planar nonlinear oscillations of elastic cables under subharmonic resonance conditions', *J. Sound Vibrat.* **132**, 1989, 367–381.
7. Szemplinska-Stupnicka, W. and Bajkowski, J., 'The 1/2 subharmonic resonance and its transition to chaotic motion in a non-linear oscillator', *Int. J. Non-Linear Mech.* **21**, 1986, 401–419.
8. Szemplinska-Stupnicka, W.,'Secondary resonance and approximate models of routes to chaotic motion in non-linear oscillators', *J. Sound Vibrat.* **113**, 1987, 155–172.
9. Thompson, J. M. T. and Stewart, H. B., *Nonlinear Dynamics and Chaos*, Wiley, Chichester, 1986.
10. Moon, F., *Chaotic Vibrations*, Wiley, New York, 1987.
11. Fang, T. and Dowell, E. H., 'Numerical simulations of periodic and chaotic responses in a stable Duffing system', *Int. J. Non-Linear Mech.* **22**, 1987, 401–425.
12. Zavodney, L. D., Nayfeh, A. H., and Sanchez, N. E., 'The response of a single-degree-of-freedom system with quadratic and cubic nonlinearities to a principal parametric resonance', *J. Sound Vibrat.* **129**, 1989, 417–442.
13. Irvine, H. K. and Caughey, T. K., 'The linear theory of free vibrations of a suspended cable', *Proc. R. Soc.* **A341**, 1974, 299–315.
14. Tongue, B. H., 'Characteristics of numerical simulations of chaotic systems', *ASME J. Appl. Mech.* **54**, 1987, 695–699.
15. Wolf, A., Swift, J., Swinney, H. L., and Vastano, J., 'Determining Lyapunov exponents from a time series', *Physica* **16D**, 1985, 285–317.

16. Frederickson, R., Kaplan, J., Yorke, E., and Yorke, J., 'The Lyapunov dimension of strange attractors', *J. Diff. Eqs.* **49**, 1983, 185.
17. Grassberger, P., and Proccacia, I., 'Characterization of strange attractors', *Phys. Rev. Lett.* **50**, 1983, 346–349.
18. Kreuzer, E. J., 'On the numerical study of bifurcation problems', in: Küpper, T., Seydel, R., and Troger, H. (eds.), *Bifurcations: Analysis, Algorithm, Applications*, Birkhäuser, Basel, 1987, 161–171.
19. Pezeshki, C. and Dowell, E. H., 'Generation and analysis of Lyapunov exponents for the buckled beam', *Int. J. Non-Linear Mech.* **24**, 1989, 79–97.
20. Moon, F. C. and Li, G. X., 'The fractal dimension of the two-well potential strange attractor', *Physica* **17D**, 1985, 99–108.
21. Zavodney, L. D. and Nayfeh, A. H., 'The response of a single-degree-of-freedom system with quadratic and cubic non-linearities to a fundamental parametric resonance', *J. Sound Vibrat.* **120**, 1988, 63–93.
22. Collett, P. and Eckmann, J. P., *Iterated Maps on the Interval as Dynamical Systems*, Birkhäuser, Boston, 1980.
23. Lauterborn, W. and Cramer, E., 'Subharmonic route to chaos observed in acoustics', *Phys. Rev. Lett.* **47**, 1981, 1445–1448.